CRYSTAL GROWTH & DESIGN

pubs.acs.org/crystal

Article

Growth Advancement of GaAs-Based BGaInAs Alloys Emitting at 1.3 μm by Molecular Beam Epitaxy

Rasha H. El-Jaroudi, Kyle M. McNicholas, Herbert S. Mączko, Robert Kudrawiec, and Seth R. Bank*

Cite This: https://doi.org/10.1021/acs.cgd.2c00131

Read Online

ACCESS | Metrics & More | Article Recommendations

ABSTRACT: Owing to the small lattice constants of the boron pnictides, strain engineering through the introduction of boron into compressively strained III−V alloys could enable both wavelength extension of GaAs-based emitters and absorbers, as well as coherent growth of direct bandgap III−V materials on silicon. Here, we systematically investigate the growth of BGaInAs alloys by molecular beam epitaxy and identify a highly kinetically limited growth regime that promotes substitutional incorporation of boron in BGaInAs alloys grown on GaAs, enabling synthesis of $B_{0.10}Ga_{0.42}In_{0.48}As$, the highest simultaneous incorporation of boron and indium yet reported in the literature. The effects of this optimized growth regime on the boron incorporation and optical properties of BGaInAs alloys were investigated; specifically, the growth rate, arsenic overpressure, and substrate temperature were found to substantially affect the boron incorporation and material quality. The optimized growth regime presented results in near-unity substitutional incorporation of boron as well as improved photoluminescence yield with the addition of boron, as opposed to the material degradation commonly observed in highly mismatched alloys.

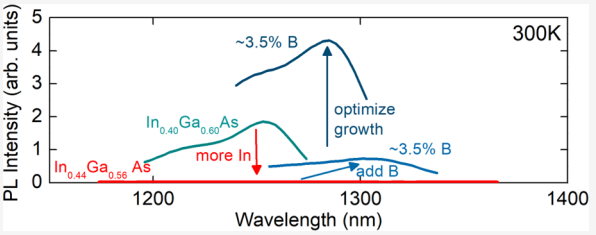

INTRODUCTION

The realization of near-infrared GaAs-based optoelectronic devices utilizing conventional III−V materials remains limited by the lack of available alloys lattice-matched or nearly lattice-matched to GaAs. This limitation has motivated the exploration of highly mismatched dilute-nitride and dilute-bismide alloys for near-infrared III−V devices on GaAs; however, their realization remains challenging owing to the limited solubility of both N and Bi in conventional zinc-blende III−V alloys. Alternatively, the potential for near-infrared optoelectronic devices on silicon and GaAs by leveraging the small lattice constant of zinc-blende boron pnictides has been well established.[1−3] The incorporation of boron in conventional III−V alloys appears promising due to predictions of increased solid solubility in these alloys compared to nitrogen.[2] While up to 15 and 8% boron incorporation in the ternary BGaAs has been demonstrated by molecular beam epitaxy (MBE)[3] and MOCVD,[4] respectively, boron incorporation in the quaternary alloy BGaInAs has thus far been limited to <4%.[1,5,6] Previous investigations of the 'dilute borides' and of other highly mismatched alloys such as the dilute nitrides and dilute bismides have demonstrated that precise control of growth parameters is critical to the promotion of substitutional incorporation of the highly mismatched constituent, often necessitating a highly kinetically limited growth regime including optimized growth rate,[7,8] substrate temperature,[9−12] and group-V overpressure.[9] Under unoptimized growth conditions, boron incorporation in the ternary alloy BGaAs was similarly limited to <4% B, and B was reported to be incorporated interstitially[9,12] and on antistites,[13,23] or phase separation of B was observed.[14,15] Molecular beam epitaxy enables independent control of these growth parameters, simplifying control of surface kinetics and providing a method to overcome the thermodynamic limitations of highly mismatched III−V alloy growth.

Here, we focused on improving the quality of BGaInAs alloys with elevated B and In contents to extend the wavelengths available lattice-matched or nearly lattice-matched to GaAs; through careful control of the MBE growth regime, we identified a highly kinetically limited MBE growth regime that enables the substitutional incorporation of boron in BGaInAs on GaAs substrates. However, unlike previous studies of BGaAs and BGaInAs growth regimes, we focused on improving the optical quality of BGaInAs alloys through the optimization of the MBE growth regime as measured by photoluminescence efficiency. Through this optimization focused on increasing PL efficiency, we observed that high structural quality alone did not predict high optical quality. To demonstrate the applicability of these alloys for near-IR optoelectronic devices, we optimized the optical quality of

Received: January 29, 2022
Revised: April 20, 2022

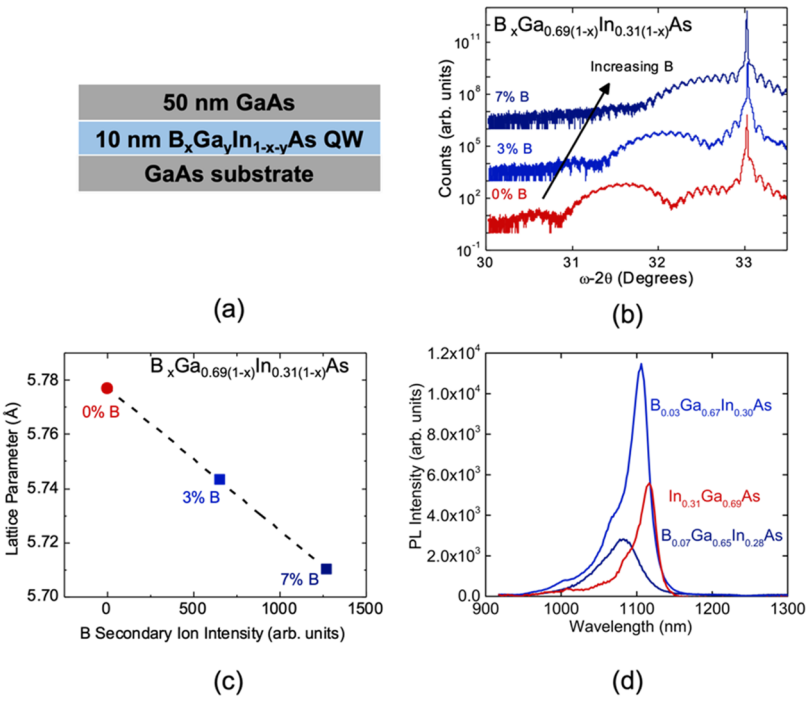

Figure 1. (a) Sample structure and (b) HR-XRD ω-2θ scans of (B)GaInAs QW with an In/Ga flux ratio of 31:69 and boron concentrations from 0 to 7%. (c) Linear relationship between change in lattice parameter measured by HR-XRD and boron secondary ion yield measured by secondary-ion mass spectrometry (SIMS) indicates near-unity substitutional incorporation. (d) Photoluminescence of the $In_{0.31}Ga_{0.69}As$, $B_{0.03}Ga_{0.67}In_{0.3}As$, and $B_{0.07}Ga_{0.64}In_{0.29}As$ QWs showed a 2× improvement in PL intensity with the addition of 3% boron, but a reduction in PL intensity and peak broadening with the addition of 7% boron.

BGaInAs quantum well structures emitting at 1.3 μm, a technologically relevant wavelength with applications in telecommunications and LIDAR. We then focused on further increasing the B and In concentrations to target longer-wavelength emitters and overcome the observed blueshift in emission from unintentional *in situ* annealing observed during the extended growths necessary for device structures.[16]

RESULTS AND DISCUSSION

Previous limitations associated with B incorporation in BGaAs were overcome through a highly kinetically limited growth regime defined by McNicholas et al.[3] combining disparate observations from prior investigations of BGaAs growth, specifically employing fast growth rates,[8] low growth temperatures,[9,12] high As/group-III flux ratios,[9] and bismuth as a surfactant.[12] As reported by McNicholas et al.,[3] this growth regime enables near-unity substitutional incorporation of boron in BGaAs. Extending this growth regime to the quaternary BGaInAs decouples the alloy bandgap from lattice constant, enabling strain engineering of emitters and detectors over a range of operating wavelengths on GaAs. However, the addition of In increases the difference in lattice constant, which may increase the enthalpy of mixing compared to the In-free alloy, resulting in a more complicated growth regime.[17] We first investigated the applicability of maintaining unity substitutional incorporation of B with the addition of In, through the growth of BGaInAs quantum wells (QW) with 30% In.

Determining the constituent concentrations in quaternary alloys is not trivial, requiring pregrowth calibration of In, Ga, and B fluxes versus cell temperatures (for In, Ga) and electron-beam power (for B) using a combination of *in situ* beam-equivalent pressure (BEP) measurements and post-growth high-resolution X-ray diffraction (HR-XRD) ω-2θ scans. To calibrate the In and Ga incorporation rate, InGaAs/GaAs superlattices were grown by varying the In cell temperature. The incorporated In and Ga fluxes were calibrated to pregrowth *in situ* BEP measurements of the In and Ga effusion cells using dynamic X-ray scattering simulations to determine the alloy composition and thickness from HR-XRD ω-2θ measurements of the superlattice samples. Owing to the unity substitutional incorporation of these elements under group-III limited growth regimes,[18] we assumed that the incorporation of Ga and In did not change with the addition of B and used these flux calibrations to control the In/Ga flux ratios during the growth of quaternary BGaInAs alloys. Eutectic reactions between elemental boron and the tungsten filament of the ionization gauge[19] used for BEP measurements precludes *in situ* BEP measurements of the B evaporator. Instead, a series of BGaAs films were grown with varying e-beam power and dynamic X-ray scattering simulations of HR-XRD ω-2θ measurements were used to determine the substitutional incorporation of B. The Arrhenius relationship between incorporated B flux (measured by HR-XRD) and B e-beam evaporator power observed in BGaAs alloys enabled calibration of B flux as a function of evaporator power prior to growth.[3] Similar to the method demonstrated in the dilute nitrides by Spruytte et al.[20] and extended for BGaAs by McNicholas et al.,[3] we observed a linear relationship between measured incorporated B in HR-XRD and the B secondary ion yield (Figure 1b) measured by secondary-ion mass spectrometry (SIMS) in our quaternary BGaInAs alloys, consistent with near-unity substitutional B incorporation with the addition of In, validating the assumptions outlined above.

Photoluminescence (PL), shown in Figure 1d, measured from the $In_{0.31}Ga_{0.69}As$ QW, $B_{0.03}Ga_{0.67}In_{0.3}As$ QW, and

https://doi.org/10.1021/acs.cgd.2c00131
Cryst. Growth Des. XXXX, XXX, XXX−XXX

$B_{0.07}Ga_{0.64}In_{0.29}As$ structures shown in Figure 1a showed an ~2× improvement in PL intensity with the addition of 3% boron and a small blueshift in wavelength, demonstrating that the addition of boron does not inherently preclude optical quality material and may in fact be used to improve the optical quality of near-IR emitters on GaAs. However, when increasing the B concentration to 7%, we observed a decrease in PL intensity as well as broadening of the PL emission spectrum. Similarly, we observed a decrease in PL intensity at higher In concentrations,[16] which motivated our investigation of optimal molecular beam growth kinetics on material quality.

Epilayer growth rate has been previously shown to affect both the surface roughness and structural quality of BGaAs films.[8] However, the influence of growth rate on the optical quality of BGaInAs alloys has not been studied in detail. Jasik et al. observed an increase in PL intensity in MBE-grown InGaAs QWs with increasing growth rate, until an optimal point after which the PL efficiency began to decrease.[21] Probing the effect of growth rate on the optical quality of BGaInAs alloys, we grew QW structures (Figure 1a), maintaining an In/Ga flux ratio of ~44:56, varying the B concentration from 2 to 4% and varying the BGaInAs growth rate from 2 to 2.8 Å/s. As shown in Figure 2, PL measurements

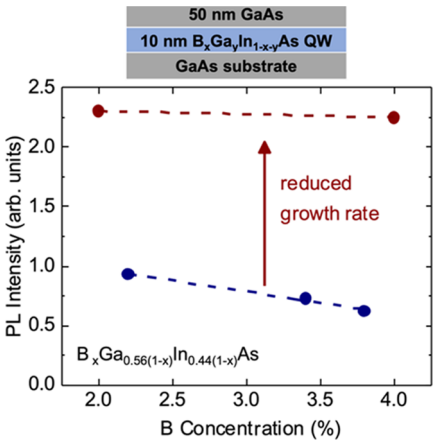

Figure 2. Photoluminescence intensity of $B_xGa_{0.56(1-x)}In_{0.44(1-x)}As$ grown at 2 Å/s (red curve) and 2.8 Å/s (blue curve). Slower growth rate resulted in improved overall PL intensity and mitigated the apparent decrease in PL intensity with increasing B concentration as seen at a higher growth rate.

from these QWs indicate that growth at 2 Å/s improves the alloy optical quality, with an ~2× increase in PL intensity observed for the 2% B QW. The impact of growth rate on optical quality increased as the B concentration was increased to 4% B, with an ~4× increase in PL intensity observed in the 4% BGaInAs QW.

Interestingly, the perceived "B penalty" decrease in PL intensity with increasing B in samples grown at 2.8 Å/s was not observed in the QW structures grown at 2 Å/s. Previous studies suggest that epitaxial growth kinetics extend beyond the immediate sample surface, with rearrangement of atoms occurring between the surface and top 4−10 atomic layers during MBE growth.[18,22] The number of monolayers participating in the rearrangement may be dependent on MBE growth parameters.[18] Here, we believe that the slower growth rate may allow more time for a favorable rearrangement of adatoms, potentially mitigating the formation of B-related point defects,[23] which could impact the material optical quality at quantities below the detection limit of structural characterization techniques such as HR-XRD.

Growth temperature has been identified as a crucial growth parameter for boron incorporation in the dilute borides[3,9,12] as well as for promoting good structural and/or optical quality material other highly mismatched alloy growth, including in the dilute bismides[7] and dilute nitrides.[10] In the dilute borides, lower growth temperature results in increased substitutional B concentrations[3,9,12] and improved structural quality.[3] Investigating the impact of substrate temperature during growth, we grew a series of BGaInAs QW structures (Figure 1a) maintaining an In/Ga flux ratio of 44:56. As shown in Figure 3a, the loss of well-defined finite-thickness fringes in HR-XRD

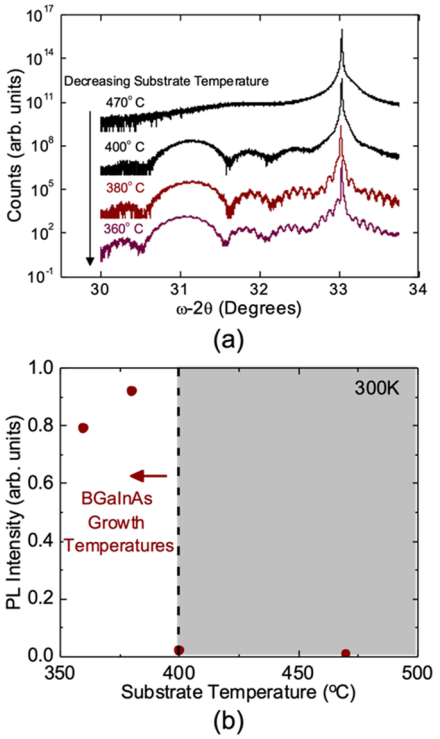

Figure 3. Low substrate temperature (<400 °C) was critical for good structural and optical quality $B_{0.03}Ga_{0.55}In_{0.42}As$ QWs. Decreasing the substrate temperature resulted in (a) improved structural quality as shown in ω-2θ scans by the reemergence of well-defined thickness fringes and QW peak and (b) improved optical quality with poor optical quality observed for samples grown at temperatures >400 °C as indicated by the lack of measurable PL.

scans as the substrate growth temperature was increased to ≥400 °C is consistent with degraded structural quality at elevated growth temperatures. Unsurprisingly, this loss of structural quality was mirrored in the optical quality of the material and no measurable PL was observed in samples grown at temperatures ≥400 °C (Figure 3b). Based on our observations of PL intensity versus growth temperature, 380 °C is the optimal growth temperature for these BGaInAs alloys.

Building on the improvements in optical quality observed at slower growth rates, we sought to optimize the V/III flux ratio to further improve the optical quality of BGaInAs emitters. As with the alloy growth rate, previous investigations of the group-V/III flux ratio in B alloy growth have primarily focused on promoting substitutional B incorporation, with virtually no reports of the impact of V/III flux ratio on the optical quality

https://doi.org/10.1021/acs.cgd.2c00131
Cryst. Growth Des. XXXX, XXX, XXX−XXX

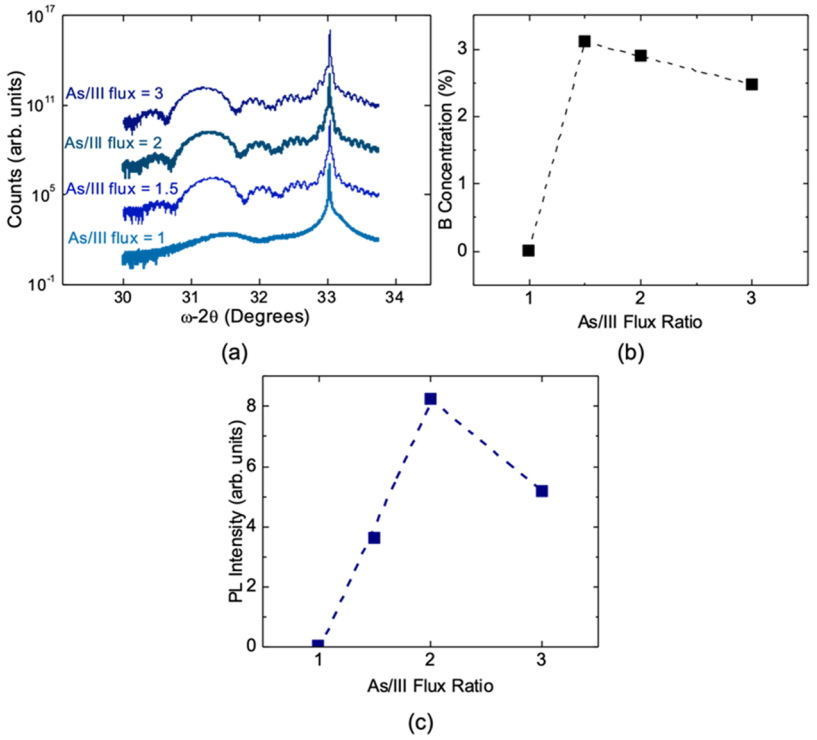

Figure 4. (a) HR-XRD ω-2θ scans of $B_{0.025}Ga_{0.55}In_{0.425}As$ QWs growth with As/III flux ratios of *ca.* 1−3. (b) A small dependence in incorporated B concentration on As/III flux ratio was measured by HR-XRD; however, the structural quality of all films grown with an As/III flux ratio >1 is comparable. (c) A strong dependence on As/III flux ratio was observed in photoluminescence.

of BGaInAs emitters. BGaInAs QW structures (Figure 1a) were grown with constant Ga, In, and B fluxes and the As_2/III flux ratio was varied from approximately 1−3. As shown in Figure 4a, HR-XRD ω-2θ measurements of the QW structures grown with an As/III flux ratio >1 showed clear QW layer diffraction peaks with pronounced finite-thickness fringes from both the QW and GaAs barrier, indicating high structural quality. Groenert et al. previously demonstrated increased substitutional B incorporation in BGaAs films with increasing As_4/III flux ratio.[9] Contrary to the findings of Groenert et al. for BGaAs films,[9] we noted a small decrease (∼0.5%) in B incorporation with increasing As_2 overpressure as seen in Figure 4c (samples were grown out of order). We employed Bi as a surfactant, a lower growth temperature, and As_2 rather than As_4. Lower growth temperatures[24] and an As_2 (instead of As_4) overpressure[25,26] have been shown to decrease adatom surface migration, which may explain the difference. Further investigation is necessary to understand the effects of As_2/III ratio on B incorporation in BGaAs and BGaInAs alloys under these growth conditions.

Additionally, as shown in Figure 4b, despite the consistent high structural quality observed in HR-XRD, varying the As/III flux ratio significantly impacted the QW PL intensity. At low substrate temperatures, such as those required for BGa(In)As growth, high As/III flux ratios promote As-related point defects, which behave as nonradiative recombination centers, decreasing direct band-to-band recombination of carriers and reducing the optical quality of the material.[27] Because low substrate temperatures are necessary to promote substitutional incorporation of B in BGaInAs alloys, the As/III overpressure needs to be carefully balanced so that enough As is supplied to avoid V-site vacancies while also minimizing the formation of As-related point defects from an excess As_2.[18] Our PL measurements indicate that an As/III flux ratio of ∼2 resulted in the highest photoluminescence intensity. This As/III flux ratio has similarly been found to result in peak luminescence efficiencies in previous investigations of GaAs and AlGaAs alloys grown by MBE.[18,28−30]

Combining these disparate growth optimizations, we grew a QW structure with a BGaInAs growth rate of 2 Å/s, a growth temperature of 380 °C, and an As_2/III flux ratio of ∼2. The growth optimized structure showed a 10× improvement in PL intensity over a control sample grown under the initial BGaAs growth conditions of a fast growth rate of 2.8 Å/s, a growth temperature of 380 °C, and an As_2/III flux ratio of ∼3. As shown in Figure 5, these growth optimizations facilitated improvement in the BGaInAs optical quality such that the B-containing QW grown under these conditions exhibited significantly increased PL efficiency over B-free InGaAs QWs

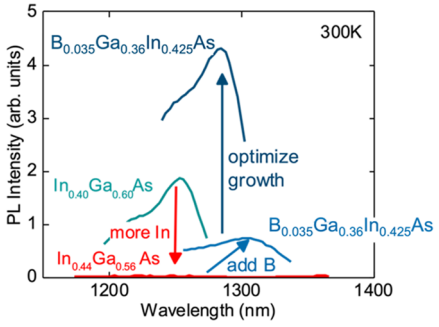

Figure 5. Refining the growth of BGaInAs QWs focused on improving the optical quality of the material through control of surface kinetics resulted in increased PL efficiencies compared to boron-free InGaAs QWs of similar and reduced In concentrations.

https://doi.org/10.1021/acs.cgd.2c00131
Cryst. Growth Des. XXXX, XXX, XXX−XXX

with both comparable and reduced In concentrations. As discussed in our previous report detailing strain engineering in BGaInAs alloys, the addition of boron to high-In-concentration InGaAs QWs reduces the lattice mismatch with the underlying GaAs substrate, preventing the formation of PL-degrading strain-related defects.[16] Here, we demonstrate that careful optimization of BGaInAs alloy growth enables not only wavelength extension of emitters on GaAs through strain engineering but also improved optical quality at these extended wavelengths.

Understanding the B-miscibility gap in BGaInAs alloys is essential for identifying prospective device applications of these alloys as extended wavelength emitters/absorbers on GaAs. Likewise, with at least 25% B necessary to lattice-match these alloys to Si, establishing the miscibility limits of B in BGaInAs is critical to evaluating the potential of these materials for the realization of direct-gap BGaInAs alloys on Si. To further probe the miscibility limit of B in BGaInAs, we grew additional BGaInAs QW structures simultaneously increasing the In/Ga flux ratio and the B flux while maintaining the growth conditions optimized at 1.3 μm (380 °C substrate temperature, Bi as a surfactant, As_2/III flux ratio of ~2, and a GaAs growth rate of ~2 Å/s). As shown in Figure 6a, increasing the In/Ga flux ratio to ~53:47 from ~44:56 resulted in the broadening of the BGaInAs QW layer peak as well as the disappearance of finite-thickness fringes in high-resolution HR-XRD ω-2θ scans, indicating degraded structural properties, even under our previously optimized growth regime. Consistent with reports of growth optimization in dilute nitrides[31] and dilute bismides,[7] the optimal growth window for substitutional boron incorporation may narrow and/or shift as the In or B concentration is increased and the alloy becomes more highly mismatched.

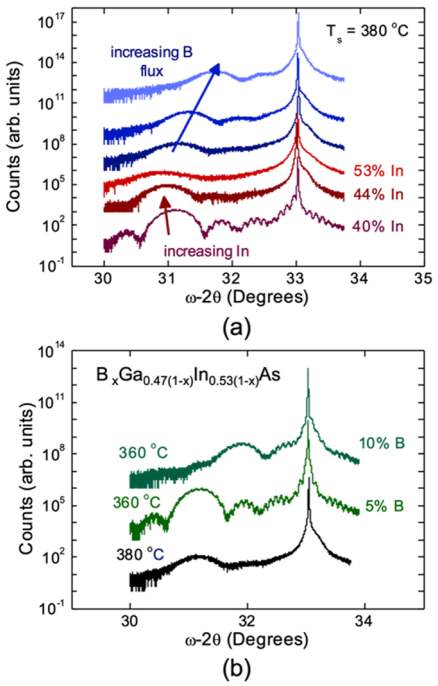

Figure 6. (a) HR-XRD ω-2θ scans indicate structural degradation was observed in BGaInAs QWs with an In/Ga flux ratio of 53:47, which were grown under the optimized conditions previously established for BGaInAs QWs with an In/Ga flux ratio of 44:56. (b) Lowering the substrate temperature to 360 °C, high structural quality was observed with BGaInAs layers incorporating up to 10% B.

To investigate the potential narrowing and shifting of the optimal growth regime, we returned to the growth regime established by McNicholas et al.[3] for BGaAs (growth rate of ~2.8 Å/s, growth temperature of 380 °C, As/III flux ratio of ~3) and found that decreasing the growth temperature of BGaInAs QWs to 360 °C with an In/Ga ratio of 53:47 to 360 °C resulted in increased substitutional B incorporation and good structural quality, as shown in Figure 6b. The observed sensitivity of structural quality to substrate growth temperature with increasing In/B concentration further emphasizes the importance of substrate temperature on BGaInAs alloy quality and indicates this growth parameter as a good starting point for the optimization of yet unexplored alloys with different In/B concentrations. The photoluminescence of these alloys with high In and B concentrations is discussed in ref.[16]

CONCLUSIONS

We have demonstrated an optimized MBE growth regime for achieving high-optical-quality BGaInAs alloys. While prior investigations of BGaInAs growth using MBE focused primarily on controlling surface kinetics to promote boron incorporation, we demonstrated here that high structural quality does not necessarily correlate to high optical quality, which is critical to the realization of BGaInAs optoelectronic devices. In particular, we demonstrated enhanced optical quality in BGaInAs QW structures over boron-free control structures through growth space optimization by reducing the BGaInAs growth rate, substrate growth temperature, and V/III flux ratio established in prior BGaAs growth optimizations, which focused on increasing boron incorporation. These advancements highlight the potential for BGaInAs-active-region devices on both GaAs and Si for applications in LiDAR, telecommunications, and quantum information processing. Additionally, we further probed the ultimate miscibility of BGaInAs alloys and observed an increase in sensitivity of the alloy structural quality to substrate temperature with increasing In/Ga flux ratio, indicating narrowing of the optimal BGaInAs growth regime and suggesting that the alloy becomes more highly mismatched as the In concentration is increased. Through further growth refinement, we demonstrated the growth of $B_{0.1}Ga_{0.42}In_{0.48}As$, which incorporated the highest simultaneous concentrations of B and In yet reported.

EXPERIMENTAL METHODS

The samples in this study were grown using solid-source molecular beam epitaxy (MBE) in an EPI Mod Gen II system equipped with a Veeco Mark IV valved cracker for arsenic, Veeco dual filament SUMO effusion cells for gallium and indium, and an MBE Komponenten electron-beam evaporation boron source for boron. The substrate temperature was measured by optical pyrometry, with a wavelength response centered at 960 nm to improve the accuracy of low-temperature measurements. The pyrometer temperature was calibrated at a growth temperature of 580 °C by heating a bare GaAs wafer and observing thermal desorption of the native oxide with reflection high-energy electron diffraction (RHEED). Photoluminescence (PL) structures with a 10 nm BGaInAs QW and a 50 nm GaAs cap were grown on semi-insulating (100) GaAs substrates with a 200 nm GaAs buffer, as shown in Figure 1a. Photoluminescence structures were designed to facilitate the optimization of the optical quality of the BGaInAs layer. The GaAs buffer layer was grown with an As_2/Ga flux ratio of 3 (beam-equivalent pressure ratio of 15). The first 100

https://doi.org/10.1021/acs.cgd.2c00131
Cryst. Growth Des. XXXX, XXX, XXX−XXX

nm of the buffer was grown at 600 °C. During the following 100 nm, the sample was cooled to the BGaInAs growth temperature (typically <400 °C). The GaAs growth rates employed were between 1 and 1.3 Å/s. The BGaInAs growth rates used were approximately 2−3 Å/s. The group-V/III flux ratio was approximated by modifying the method of Svensson et al.,[32] the group-V BEP, where the transition from group-III to group-V limited RHEED oscillations was identified corresponding to the 1:1 incorporation point of group-III and group-V atoms. High-resolution X-ray diffraction ω-2θ coupled scans were performed about the (004) diffraction peak of GaAs using a Rigaku SmartLab HR-XRD. Rigaku Global Fit Dynamic X-ray scattering simulations were used to fit layer compositions and strain. The composition of the quaternary alloys was interpolated from ternary composition calibrations of InGaAs and BGaAs, as described in the manuscript. The room-temperature photoluminescence reported in Figure 1 was measured using a 532 nm Nd:YAG diode-pumped solid-state laser and a Hamamatsu TG-cooled NIR-I mini spectrometer. The room-temperature photoluminescence was measured using a chopped 532 nm Nd:YAG diode-pumped solid-state laser at ∼100 mW of power at the sample, a 0.5 mm grating spectrometer, and a thermoelectric-cooled InGaAs detector with the output measured via an SRS-830 lock-in amplifier. Time-of-flight secondary-ion mass spectrometry (TOF-SIMS) was performed in an ION-TOF-GmbH with Bi as the primary ion and Cs as the secondary ion.

AUTHOR INFORMATION

Corresponding Author

Seth R. Bank − *Electrical and Computer Engineering, University of Texas at Austin, Austin 78758 Texas, United States;* orcid.org/0000-0002-5682-0126; Email: sbank@utexas.edu

Authors

Rasha H. El-Jaroudi − *Electrical and Computer Engineering, University of Texas at Austin, Austin 78758 Texas, United States*

Kyle M. McNicholas − *Electrical and Computer Engineering, University of Texas at Austin, Austin 78758 Texas, United States;* orcid.org/0000-0002-2426-2027

Herbert S. Mączko − *Department of Semiconductor Materials Engineering, Faculty of Fundamental Problems of Technology, Wroclaw University of Science and Technology, Wroclaw 50-370, Poland*

Robert Kudrawiec − *Department of Semiconductor Materials Engineering, Faculty of Fundamental Problems of Technology, Wroclaw University of Science and Technology, Wroclaw 50-370, Poland;* orcid.org/0000-0003-2593-9172

Complete contact information is available at: https://pubs.acs.org/10.1021/acs.cgd.2c00131

Notes

The authors declare no competing financial interest.

ACKNOWLEDGMENTS

This work was performed in part at the University of Texas Microelectronics Research Center, a member of the National Nanotechnology Coordinated Infrastructure (NNCI), which is supported by the National Science Foundation (no. ECCS-1542159). This work was also supported by the National Science Foundation (Award Nos. ECCS-1933836, ECCS-2133187, and ECCS-2133195). The authors thank Andrei Dolocan for assistance in performing secondary-ion mass spectrometry measurements. R.H.E. acknowledges fellowship support from NXP Semiconductors and Texas Instruments.

REFERENCES

(1) Geisz, J. F.; Friedman, D. J.; Olson, J. M.; Kurtz, S. R.; Reedy, R. C.; Swartzlander, A. B.; Keyes, B. M.; Norman, A. G. BGaInAs alloys lattice matched to GaAs. *Appl. Phys. Lett.* **2000**, *76*, 1443−1445.

(2) Hart, G. L. W.; Zunger, A. Electronic structure of BAs and boride III-V alloys. *Phys. Rev. B* **2000**, *62*, 13522−13537.

(3) McNicholas, K. M.; El-Jaroudi, R. H.; Bank, S. R. Kinetically limited molecular beam epitaxy of $B_xGa_{1-x}As$ alloys. *Cryst. Growth Des.* **2021**, *21*, 6076−6082.

(4) Hamila, R.; Saidi, F.; Rodriguez, P. H.; Auvray, L.; Monteil, Y.; Maaref, H. Growth temperature effects on boron incorporation and optical properties of BGaAs/GaAs grown by MOCVD. *J. Alloys Compd.* **2010**, *506*, 10−13.

(5) Hamila, R.; Saidi, F.; Maaref, H.; Rodriguez, P.; Auvray, L. Photoluminescence properties and high resolution x-ray diffraction investigation of BInGaAs/GaAs grown by the metalorganic vapour phase epitaxy method. *J. Appl. Phys.* **2012**, *112*, No. 063109.

(6) Wang, Q.; Jia, Z.; Ren, X.; Yan, Y.; Bian, Z.; Zhang, X.; Cai, S.; Huang, Y. Effect of boron incorporation on the structural and photoluminescence properties of highly-strained $In_xGa_{1-x}As$/GaAs multiple quantum wells. *AIP Adv.* **2013**, *3*, No. 072111.

(7) Ptak, A. J.; France, R.; Beaton, D. A.; Alberi, K.; Simon, J.; Mascarenhas, A.; Jiang, C. S. Kinetically limited growth of GaAsBi by molecular-beam epitaxy. *J. Cryst. Growth* **2012**, *338*, 107−110.

(8) Detz, H.; MacFarland, D.; Zederbauer, T.; Lancaster, S.; Andrews, A. M.; Schrenk, W.; Strasser, G. Growth rate dependence of boron incorporation into $B_xGa_{1-x}As$ layers. *J. Cryst. Growth* **2017**, *477*, 77−81.

(9) Groenert, M. E.; Averbeck, R.; Hösler, W.; Schuster, M.; Riechert, H. Optimized growth of BGaAs by molecular beam epitaxy. *J. Cryst. Growth* **2004**, *264*, 123−127.

(10) Bank, S. R.; Yuen, H. B.; Wistey, M. A.; Lordi, V.; Bae, H. P.; Harris, J. S. Effects of growth temperature on the structural and optical properties of 1.55 μm GaInNAsSb quantum wells grown on GaAs. *Appl. Phys. Lett.* **2005**, *87*, No. 021908.

(11) Kong, X.; Trampert, A.; Tournié, E.; Ploog, K. H. Decomposition in as-grown (Ga,In)(N,As) quantum wells. *Appl. Phys. Lett.* **2005**, *87*, No. 171901.

(12) Ptak, A. J.; Beaton, D. A.; Mascarenhas, A. Growth of BGaAs by molecular-beam epitaxy and the effects of a bismuth surfactant. *J. Cryst. Growth* **2012**, *351*, 122−125.

(13) Tischler, M. A.; Mooney, P. M.; Parker, B. D.; Cardone, F.; Goorsky, M. S. Metalorganic vapor phase epitaxy and characterization of boron-doped (Al,Ga)As. *J. Appl. Phys.* **1992**, *71*, 984−992.

(14) Geisz, J.; Friedman, D.; Kurtz, S.; Olson, J.; Swartzlander, A.; Reedy, R.; Norman, A. Epitaxial growth of BGaAs and BGaInAs by MOCVD. *J. Cryst. Growth* **2001**, *225*, 372−376.

(15) Dumont, H.; Rutzinger, D.; Vincent, C.; Dazord, J.; Monteil, Y.; Alexandre, F.; Gentner, J. L. Surface segregation of boron in BxGa1-xAs/GaAs epilayers studied by x-ray photoelectron spectroscopy and atomic force microscopy. *Appl. Phys. Lett.* **2003**, *82*, 1830−1832.

(16) El-Jaroudi, R. H.; McNicholas, K. M.; Briggs, A. F.; Sifferman, S. D.; Nordin, L.; Bank, S. R. Room-temperature photoluminescence and electroluminescence of 1.3- μm-range BGaInAs quantum wells on GaAs substrates. *Appl. Phys. Lett.* **2020**, *117*, No. 021102.

(17) Stringfellow, G. B. Thermodynamic considerations for epitaxial growth of III/V alloys. *J. Cryst. Growth* **2017**, *468*, 11−16.

(18) Larkins, E. C.; Harris, J. S. Molecular Beam Epitaxy of High-Quality GaAs and AlGaAs. In *Molecular Beam Epitaxy*, Farrow, R. F. C., Ed.; William Andrew Inc., 1995; pp 114−274.

(19) Duschanek, H.; Rogl, P. Critical Assessment and Thermodynamic Calculation of the Binary System Boron-Tunsten (B-W). *J. Phase Equilib.* **1995**, *16*, 150−161.

(20) Spruytte, S. G.; Coldren, C. W.; Marshall, A. F.; Larson, M. C.; Harris, J. S. MBE Growth of Nitride-Arsenide Materials for long Wavelength Opto-electronics. *MRS Internet J. Nitride Semicond. Res.* **2000**, *5*, 474−480.

(21) Jasik, A.; Wnuk, A.; Gaca, J.; Wójcik, M.; Wójick- Jedlińska, A.; Muszalski, J.; Strupiński, W. The influence of the growth rate and V/III ratio on crystal quality of InGaAs/GaAs QW structures by MBE and MOCVD methods. *J. Cryst. Growth* **2009**, *311*, 4423−4432.
(22) Moison, J. M.; Houzay, F.; Barthe, F.; Gérard, J. M.; Jusserand, B.; Massies, J.; Turco-Sandroff, F. S. Surface segregation in III—V alloys. *J. Cryst. Growth* **1991**, *111*, 144−150.
(23) Gupta, V. K.; Koch, M. W.; Watkins, N. J.; Gao, Y.; Wicks, G. W. Molecular beam epitaxial growth of BGaAs ternary compounds. *J. Electron. Mater.* **2000**, *29*, 1387−1391.
(24) Ibbetson, J. P. Effects of As_4 flux on reflection high-energy electron diffraction oscillations during growth of GaAs at low temperatures. *J. Vac. Sci. Technol. B* **1994**, *12*, 1050.
(25) Neave, J. H.; Dobson, P. J.; Harris, J. J.; Dawson, P.; Joyce, B. A. Silicon doping of MBE-grown GaAs films. *Appl. Phys. A: Mater. Sci. Process.* **1983**, *32*, 195−200.
(26) Ogura, T.; Kishimoto, D.; Nishinaga, T. Effect of As molecular species on inter-surface diffusion in GaAs MBE for ridge structure fabrication. *J. Cryst. Growth* **2001**, *226*, 179−184.
(27) Loka, H. S.; Benjamin, S. D.; Smith, P. W. E. Optical characterization of low-temperature-grown GaAs for ultrafast all-optical switching devices. *IEEE J. Quantum Electron.* **1998**, *34*, 1426−1437.
(28) Akimoto, K.; Kamada, M.; Taira, K.; Arai, M.; Watanabe, N. Photoluminescence killer center in AlGaAs grown by molecular-beam epitaxy. *J. Appl. Phys.* **1986**, *59*, 2833.
(29) Hayakawa, T.; Kondo, M.; Suyama, T.; Takahashi, K.; Yamamoto, S.; Yano, S.; Hijikata, T. Effect of group V/III flux ratio on deep electron traps in $Al_xGa_{1-x}As$ (x = 0.7) grown by molecular beam epitaxy. *Appl. Phys. Lett.* **1986**, *49*, 788.
(30) Wood, C. E. C.; Morgan, D. V.; Rathbun, L. Molecular-beam epitaxial group III arsenide alloys: Effect of substrate temperature on composition. *J. Appl. Phys.* **1982**, *53*, 4524.
(31) Bank, S. R.; Wistey, M. A.; Yuen, H. B.; Goddard, L. L.; Bae, H.; Harris, J. S. Molecular-beam epitaxy growth of low-threshold cw GaInNAsSb lasers at 1.5 μm. *J. Vac. Sci. Technol. B* **2005**, *23*, 1337.
(32) Svensson, S. P.; Hier, H.; Sarney, W. L.; Donetsky, D.; Wang, D.; Belenky, G. Molecular Beam Epitaxy Control and Photoluminescence Properties of InAsBi. *J. Vac. Sci. Technol., B: Nanotechnol. Microelectron.: Mater., Process., Meas., Phenom.* **2012**, *30*, No. 02B109.

https://doi.org/10.1021/acs.cgd.2c00131
Cryst. Growth Des. XXXX, XXX, XXX−XXX